The Journal of Laryngology and Otology
November 1995, Vol. **109**, pp. 1057–1060

Charing Cross CT protocol for endoscopic sinus surgery

J. ROWE-JONES, F.R.C.S., I. MACKAY, F.R.C.S., I. COLQUHOUN, F.R.C.R.*

Abstract
The Charing Cross computerized tomography protocol for imaging the paranasal sinuses uses 2 mm thick slices with table increments of 8 mm: 10 to 12 coronal and two axial images are produced. These provide the necessary information for diagnosis of chronic rhinosinusitis and safe endoscopic sinus surgery. The technique is quicker and cheaper than previously described protocols and exposes the lens of the eye to less radiation.

Key words: Rhinosinusitis, chronic; Endoscopy, surgery; Tomography, computerized axial

Introduction

The role of computerized tomography (CT) scanning in the management of a patient with rhinosinusitis is to confirm the presence of disease and demonstrate its extent. The latter information may be used to stage disease and help determine prognosis. The extremely variable anatomy of the nasal cavities and paranasal sinuses is also demonstrated, together with the relationships of vital adjacent structures. These details are of great importance to the surgeon prior to undertaking endoscopic sinus surgery. Traditional scanning techniques involve 20–25 slices (Zinreich *et al.*, 1987). Our protocol utilizes 10–12 slices (Figure 1) which, which we believe, provide the necessary anatomical and pathological detail, whilst being quicker and cheaper, and exposing the lens of the eye to less radiation.

Method

We performed a direct coronal and a limited axial series of computed tomograms. The technical details are featured in Table I. The coronal cuts extend from the anterior wall of the frontal sinus to the posterior wall of the sphenoid sinus and are 10 to 12 in number (Figure 2). Two axial cuts are performed (Figure 3), one at the level of the mid-portion of the frontal sinus to demonstrate antero-posterior depth and one just inferior to the anterior clinoid processes to demonstrate the relationship of the optic nerve to the posterior ethmoid and sphenoid sinuses. The window settings have a centre of −200 and a width of 2000 Hounsfield units.

We have measured the skin entrance doses of radiation associated with this protocol in a random sample of 15 patients undergoing CT assessment for chronic rhinosinusitis. Lithium fluoride thermoluminescent dosemeter (TLD) chips were used and were read on a Vinten Solaro TLD reader. Prior to use the TLD chips were calibrated for the scanner, batched and annealed. Calibration accuracy was plus or minus five per cent. The TLD chips were placed in heat sealable plastic sachets with two chips per sachet. Three sachets were used for each patient, one adjacent to lens of each eye and one over the thyroid. The mean dose to the lens was found to be 9.81 mGy (SD = 5.62). The mean thyroid dose was 0.55 mGy (SD = 0.31) and was an estimate of scattered radiation as the sachet lay outside the scan beam.

Discussion

Chronic rhinosinusitis (CRS) is diagnosed from a history of eight weeks of persistant sinonasal symptoms, despite medical treatment. This diagnosis will include patients demonstrating a spectrum of disease from predominantly rhinitis to predominantly sinusitis, as the nasal and sinus mucosa are rarely affected in isolation from each other. CT scanning helps to distinguish those patients with dominant sinus involvement. Recent classification stipulates that for a definitive diagnosis of CRS, sinus mucosal abnormality should be demonstrated on CT scanning four weeks after medical therapy without intervening acute infection (Lund *et al.*, 1995). It is in this group of patients that endoscopic sinus surgery is usually considered. Kennedy (1992) suggested that the extent of sinus involvement demonstrated on CT scan equates with the outcome of functional endoscopic sinus surgery when judged with post-operative nasal endoscopy. He described four prognostic groups based on the CT scan appearance.

Pre-operative examination of the CT scan pro-

From the Departments of Otorhinolaryngology and Diagnostic Radiology*, Charing Cross Hospital, London.
Accepted for publication: 6 August 1995.

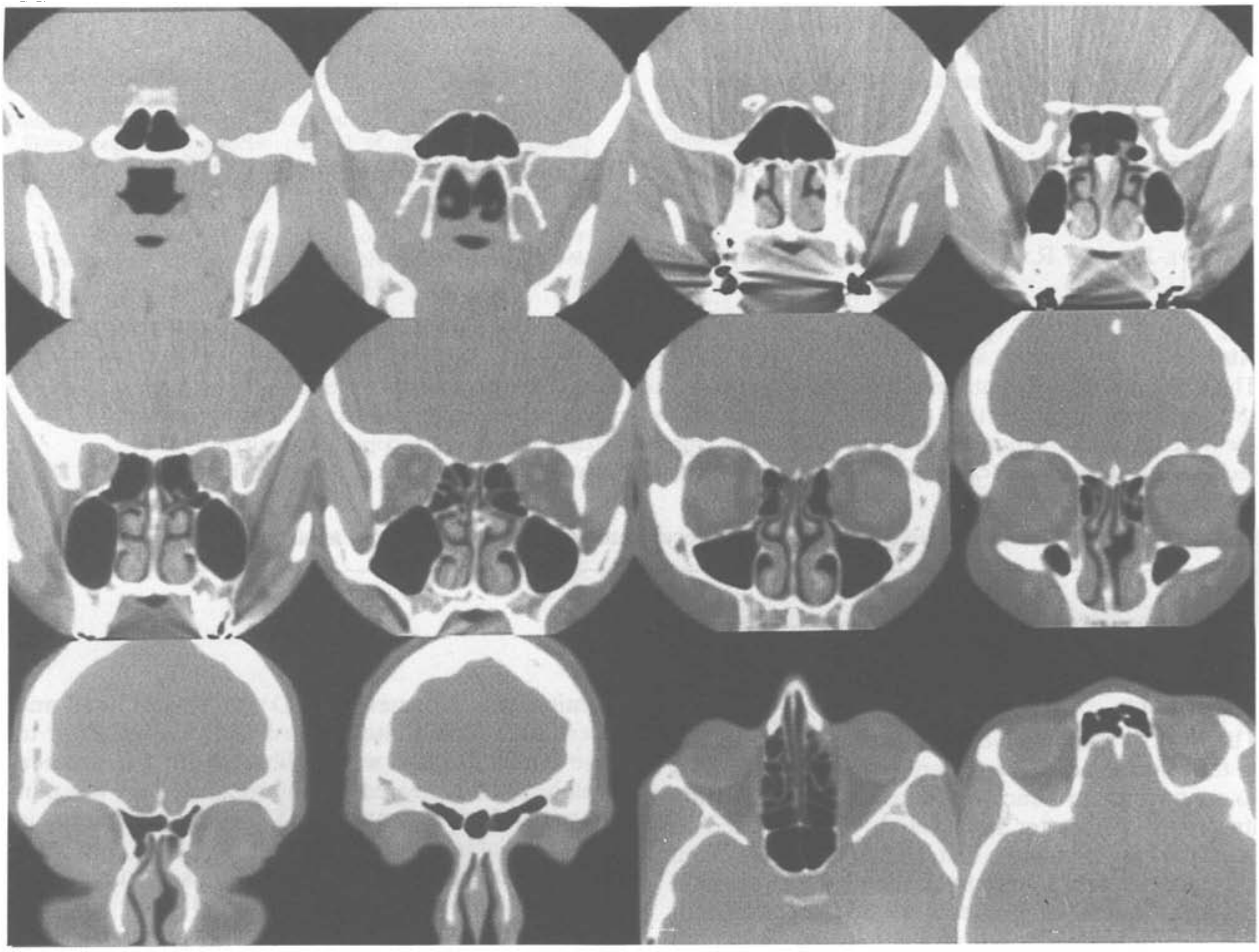

FIG. 1
Computed tomograms showing 12 slices.

vides vital anatomical information, knowledge of which makes endonasal surgery safer. Kopp and Stammberger (1991) drew particular attention to the relationship of the uncinate process with the lamina papyracea, the depth of the olfactory fossa, the presence of Onodi cells and the relationships of the sphenoid sinus to the optic nerve and internal carotid artery.

Zinreich *et al.* (1987) advocated using a CT technique of 20–25 scan images in order to provide

TABLE I
TECHNIQUE FOR CT OF THE PARANASAL SINUSES

Imaging parameter	Imaging plane: Coronal	Imaging plane: Axial
Patient position	Supine – neck extended over end of table	Supine – neck neutral
Scan plane	Perpendicular to hard palate	Parallel to hard palate
Slice thickness (mm)	2	2
Table increment (mm)	8	N/A
kV	120	120
mAs	200	200
Zoom factor	2	2
Scan time (s)	2	2
Total scanning time (min)	8	4

(N/A = not applicable).

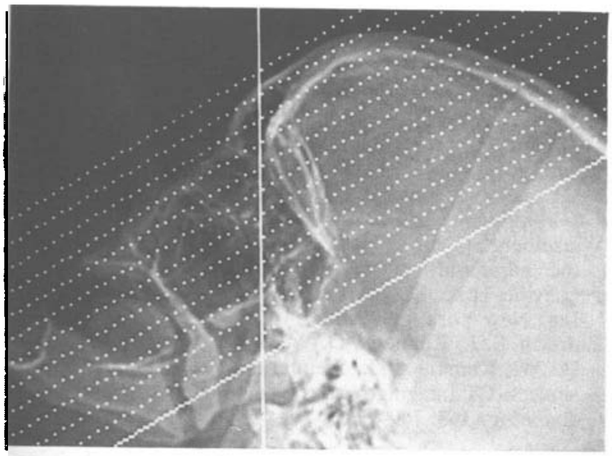

FIG. 2
Coronal cuts from anterior wall of the frontal sinus to the posterior wall of the sphenoid sinus.

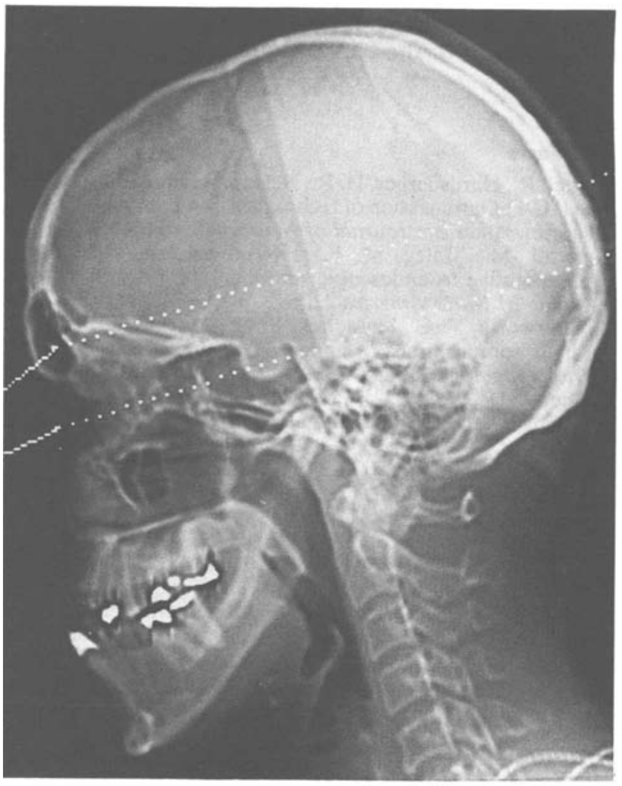

FIG. 3
Axial cuts: one at the level of the mid portion of the frontal sinus (to demonstrate anteror-posterior depth) and one just inferior to the anterior clinoid processes (to demonstrate the relationship of the optic nerve to the posterior ethmoid and sphenoid sinuses).

the precise topographical guidance needed for surgery, as well as details of disease extent and any predisposing anatomical abnormalities. This protocol involves slice thicknesses of 4 mm with 3 mm table increments. Kopp and Stammberger (1991) stated that further cuts of 2 mm thickness may be needed for extra detail in some cases: 4 mm overlapping slices will expose the lens, the most radiosensitive structure of the eye, in two to three coronal cuts. Other authors have subsequently described limited scanning techniques. Chow and Mafee (1989) used seven to eight coronal slices but no axial images. White *et al.* (1991) used six to eight coronal and two to three axial slices, 5 mm in thickness and 10 mm apart.

Our protocol uses 8 mm table increments but with a slice thickness of 2 mm. These thinner slices provide more accurate images, particularly of the ostiomeatal complex where the clefts and lamellae of the anterior ethmoid may only be 2 to 3 mm apart. Kopp and Stammberger (1991) drew attention to the artifacts of blurring inherent in tomography. Thinner slices enable better discrimination of detail, with less blurring of bony structures which might otherwise be misinterpreted as mucosal disease. Cell compartments are also better delineated. For example the agger nasi cells may be more easily distinguished from anterior extension of the bulla ethmoidalis.

Despite using fewer cuts we are still able to detect minimal disease and visualize the ostiomeatal complex. Furthermore the Charing Cross protocol also exposes the lens to less irradiation than other regimens. We cut through this structure only once in the coronal and axial planes and use a low exposure factor of 200 mAs (Babbel *et al.*, 1991).

The mean dose to the lens of the eye with our scanning protocol is 9.81 mGy. This compares with an exposure of 12 to 90 mGy associated with the CT settings used by Kopp and Stammberger (1991). More recently Maclennan (1995) assessed doses to the lens of patients undergoing CT examinations for chronic sinonasal disease in the West of Scotland. These doses were predominantly dependent upon the mAs setting of the scanner varying from 70.3 mGy at 475 mAs and 17.6 mGy at 210 mAs to 4.7 mGy at 30 mAs. The scanning protocols examined often employed greater slice widths and larger table increments than ours, which would result in loss of detail. Loss of image sharpness also occurs at lower mAs settings.

It has been argued that the main purpose of CT scanning in cases of CRS is to identify normal anatomical landmarks and variants, thereby providing a road map for safe surgery (Winzelberg *et al.*, 1993). The only relationship not always clearly displayed using our technique is the course of the internal carotid artery alongside the sphenoid sinus, in the axial plane. Our major complication rate for patients undergoing endoscopic sinus surgery, after assessment including the above described CT scanning sequence, is 0.54 per cent (Cumberworth *et al.*, 1994). These complications of an orbital haematoma and two cerebrospinal fluid leaks were not due to inadequate demonstration of anatomical detail on the CT scans. This is comparable with similar rates of 0.85 to 1.1 per cent from centres where more extensive CT protocols, similar to that described by Zinreich *et al.* (1987), are used (May *et al.*, 1993). We believe our scanning protocol enables a full and accurate assessment of the paranasal sinuses with less radiation to the lens of the eye.

References

Babbel, R., Harnsberger, H. R., Nelson, B., Sonkens, J., Hunt, S. (1991) Optimization of techniques in screening CT of the sinuses. *American Journal of Neuroradiology* **12:** 849–854.

Chow, J. M., Mafee, M. F. (1989) Radiologic assessment preoperative to endoscopic sinus surgery. *Otolaryngologic Clinics of North America* **22:** 691–701.

Cumberworth, V. L., Sudderick, R. M., Mackay, I. S. (1994) Major complications of endoscopic sinus surgery. *Clinical Otolaryngology* **19:** 248–253.

Kennedy, D. W. (1992) Prognostic factors, outcomes and staging in ethmoid sinus surgery. *Laryngoscope* **102 (suppl. 57):** 9–18.

Kopp, W., Stammberger, H. (1991) Radiology. In *Functional Endoscopic Sinus Surgery*. 1st Edition. (Stammberger, H. ed.). B. C. Decker, Philadelphia, pp 89–143.

Lund, V. J., Draf, W., Friedman, W. H., Gwaltney, J. M., Hoffman, S. R., Huizing, E. H., Jones, J. G., Jones, J. K., Kennedy, D. W., Lusk, R. P., Mackay, I. S., Moriyama, H., Naclerio, R. M., Stankiewicz, J. A., Cauwenberge, P. V., Vining, E. M. (1995) A staging classification for sinusitis. *Annals of Otology, Rhinology and Laryngology* (in Press).

Maclennan, A. C. (1995) Radiation doses to the lens from coronal CT scanning of the sinuses. *Clinical Radiology* **50:** 265–267.

May, M., Levine, H. L., Schaitkin, B., Mester, S. J. (1993) Complications of endoscopic sinus surgery. In *Endoscopic Sinus Surgery*. (Levine, H. L., May, M., eds.). Thieme Medical Publishers, Inc., New York, pp 193–203.

White, P. S., Cowan, I. A., Robertson, M. S. (1991) Limited CT scanning techniques of the paranasal sinuses. *Journal of Laryngology and Otology* **105:** 20–23.

Winzelberg , G. G., O'Hara, K., May, M. (1993) Radiology of the paranasal sinuses. In *Endoscopic Sinus Surgery*. (Levine, H. L., May, M., eds.). Thieme Medical Publishers, Inc., New York, pp 29–48.

Zinreich, S. J., Kennedy, D. W., Rosenbaum, A. E., Gayler, B. W., Kumar, A. J., Stammberger, H. (1987) Paranasal sinuses: CT imaging requirements for endoscopic surgery. *Radiology* **163:** 769–775.

Address for correspondence:
Mr J. Rowe-Jones,
Department of Otorhinolaryngology–Head and Neck Surgery,
Charing Cross Hospital,
Fulham Palace Road,
London W6 8RF.

Fax: 081 846 1070